Chemical Engineering Journal 163 (2010) 331–336

Contents lists available at ScienceDirect

Chemical Engineering Journal

journal homepage: www.elsevier.com/locate/cej

Experimental interfacial area measurements in a bubble column

R. Maceiras*, E. Álvarez, M.A. Cancela

University of Vigo, Chemical Engineering Department, E.T.S.E.I., Lagoas-Marcosende, 36310 Vigo, Spain

ARTICLE INFO

Article history:
Received 24 June 2010
Received in revised form 31 July 2010
Accepted 3 August 2010

Keywords:
Bubble column
Interfacial area
Holdup
Bubble size
Flow regimes

ABSTRACT

Gas holdup, bubble diameter and gas–liquid interfacial area were measured in a bubble column, during the absorption of CO_2 in DEA solutions in batch conditions, as a function of column height, operating time, gas flow rate and amine concentration. The experimental measurements of bubble diameter were carried out using a video technique combined with image processing. The gas flow rate was varied in the range 10–25 L/h, and the amine concentration between 0.05 and 1 M. The results show that the interfacial area is influenced with the amine concentration and gas flow rate through the column. Additionally, an empirical equation is proposed to relate the interfacial area to time and column height for each system. Furthermore, a generalized correlation based on dimensionless groups for the prediction of gas holdup in homogeneous regime was proposed and found to be in good agreement with available data.

1. Introduction

Bubble columns are widely used in industrial gas–liquid operations (e.g. gas–liquid reactions, fermentations) in chemical and biochemical processes industries, due to their simple construction, low operating cost and high-energy efficiency. In all these processes, gas holdup and bubble size are important design parameters since the gas–liquid interfacial area available for mass transfer is defined by these variables. In turn, bubble size distribution and gas holdup in gas–liquid dispersions depend largely on column geometry, type of gas sparger, operating conditions and physico-chemical properties of the two phases [1]. Furthermore, if the absorption process is accompanied by a chemical reaction, the effect of time on the interfacial area should too be analyzed.

Dispersion of the gas into the column is critical in determining the performance of gas–liquid systems. Small bubbles and a uniform distribution over the cross-section of the equipment are desirable to maximize the interfacial area and to improve the mass transfer rate [2]. For that reason, the formation of bubbles at orifices submerged in a liquid has been the subject of many theoretical and experimental works [3–5]. In the publications cited above, the main focus of research was on the bubble formation at a single orifice. However, other authors [2,6] have studied experimentally the influence of the distance between holes and of the number of holes on the bubble diameter.

Despite considerable studies of bubble column performance, many basic questions concerning the effect of important operational parameters remain unanswered. For instance, although bubble column characteristics have been studied extensively over the last few decades, there is still a fair amount of uncertainty regarding the prevailing mechanisms of bubble formation. Break-up and coalescence of fluid objects play a crucial role in a broad spectrum of multiphase flow processes such as the evolution of the bubble size distribution in stirred tanks and bubble columns [7]. Consequently, the bubble size distribution in a vessel is not constant, but rather, may change due to bubble–bubble interactions leading to breakage or coalescence. The latter is the reason why bubble size distributions measurements are not so common in literature. Moreover, almost all the published data refer to the evaluation of a mean bubble diameter inside the column usually estimated from a one-height measurement [6,8–12]. Others authors [1,2,13–17] have measured the bubble size distribution at different distances from the sparger in order to study the coalescence and breakage.

Different techniques have been developed in order to measure the bubble dimensions and shapes in equipments where gas–liquid transfer is important. Some authors have used the video technique for studying the bubble size and the gas holdup [1,2,13,14,16,17–22]. These studies were carried out in systems with air like gas phase and water, electrolyte solutions, ethanol, butanol and pentanol aqueous solutions or glycerine aqueous solutions like liquid phase. In these systems, there is no chemical reaction. Therefore, it seems interesting to contribute to a study on the subject.

In this work, the absorption process of carbon dioxide (CO_2) into diethanolamine (DEA) aqueous solutions is studied. The interfacial area and the gas holdup are measured at for several gas flow rates and several DEA concentrations. The influence of height column

* Corresponding author. Tel.: +34 986813833; fax: +34 986812201.
E-mail address: rmaceiras@uvigo.es (R. Maceiras).

1385-8947/$ – see front matter © 2010 Elsevier B.V. All rights reserved.
doi:10.1016/j.cej.2010.08.011

Nomenclature

a	interfacial area, m^{-1}
A	parameter in Eq. (12), s^{-1}
Ar	Archimedes number
d	bubble diameter, m
d_C	column diameter, m
d_{32}	Sauter mean diameter, m
e	ellipsoid minor axis, m
E	ellipsoid major axis, m
Eo	Eötvos number
Fr	Froude number
g	gravity acceleration, m s^{-2}
H_L	liquid level, m
n	number of bubbles
t	time, s
u_G	gas superficial velocity, m s^{-1}
V_L	liquid volume, m^3
w	parameter in Eq. (12), s^{-1}
x_C	parameter in Eq. (12), s^{-1}
Y_0	parameter in Eq. (12), s^{-1}

Greek symbols

ε	gas holdup
ρ	liquid density, kg m^{-3}
μ	liquid viscosity, Pa s
σ	surface tension, N m^{-1}

and operating time on interfacial area will be analyzed. The motivation for the present work was in part the small amount of work found in the literature on the study of the interfacial area variation with height column and time, since these parameters have been identified as key parameters defining the value of the volumetric mass transfer coefficient (k_La) [23].

2. Materials and methods

2.1. Experimental set-up

The experimental set-up (Fig. 1) consists of a vertical rectangular polymethyl methacrylate column 1.03 m height (1), having a square cross-section (side length 6 cm). A rectangular geometry was preferred over a cylindrical one because it simultaneously facilitates direct flow visualization and the use of optical measuring methods by minimizing optical distortion. For the injection and uniform distribution of the gas phase, a gas sparger (7), i.e., a porous plate of 4 mm in diameter was installed at the centre of the bottom plate (6). This plate has another orifice for liquid outlet (5). The top plate has three orifices: gas outlet (3), liquid inlet (2) and a thermometer (4).

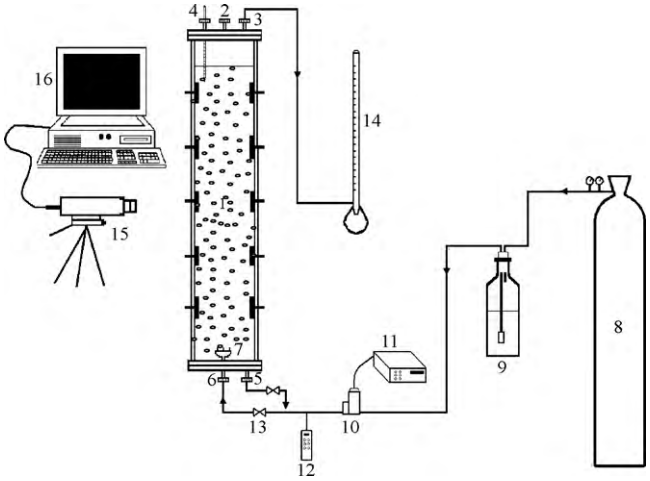

Fig. 1. Experimental set-up. (1) Bubble column; (2) liquid inlet; (3) gas outlet; (4) thermometer; (5) liquid outlet; (6) gas inlet; (7) sparger; (8) gas cylinder; (9) humidifier; (10) flow meter; (11) flow controller; (12) digital manometer; (13) gas valve; (14) soap meter; (15) video camera; (16) computer.

Aqueous diethanolamine (DEA) solutions of different concentrations were employed as liquid phase, while the gas phase was carbon dioxide with a different gas flow rate for each run. The following DEA concentrations were employed: 0.05, 0.1, 0.3 and 1.0 M. Gas flow rates of 10, 15, 20 and 25 L/h ($u_G = 7.7 \times 10^{-4}$ to 1.9×10^{-3} m/s) were used.

All the experiments were conducted at ambient pressure and temperature conditions and under batch conditions. Each experimental run was started by filling the column with appropriate liquid phase up to 100 cm above the sparger. The feed of pure carbon dioxide (8) was passed through a humidifier (9) at the ambient temperature to prepare the gas phase. This procedure removes the gas-side mass transfer, thus allowing evaluation of resistance to transfer from the gas phase to the liquid phase. The gas flow, before entering the bubble column, was metered by a flow meter (10) and controlled with a flow controller Brooks 0154 (11). All the experiments were performed with no liquid throughput, while the gas phase was injected and distributed into the liquid phase by the porous plate. Before going into the column, the pressure was measured with a digital manometer Testo 512 (12). The gas flow in the outlet was measured with a soap meter (14).

A high-speed digital video camera (SONY DCR-TRV9E) (15) was used, both, for direct flow visualization, and for the bubble size and holdup measurements. The images obtained were converted into an AVI format file using STUDIO Version 7 software (16) and processed using *UTHSCSA Image Tool* software to obtain the bubble size. The images were taken, alternatively, at three positions (20, 45 and 85 cm above the sparger) for different operating conditions until the liquid saturation was reached and therefore, the CO_2 is not already being removed. In that moment, the amount of carbon dioxide in the inlet and outlet is the same. The number of bubbles measured in each section was always higher than 30 and the standard deviation was between 0.5 and 0.7 depending on the section, gas flow rate and reaction time.

2.2. Determination of physical properties

The densities, ρ, and viscosities, μ, of the different solutions were measured at 20, 25 and 30 °C using a Anton Paar DSA 5000 densimeter, with a precision of $\pm 10^{-5}$ g cm^{-3}, and a Shott-Gëratte AVS 350 automatic viscometer, with a precision of ±0.01 s, respectively. The experimental values were correlated simultaneously with the amine concentration and with the temperature, obtaining the following expressions:

$$\rho = 12.26 \cdot C_{B_0} + 915.65 \cdot \exp^{25.3/T} \quad (1)$$

$$\ln \mu = 0.3 \cdot C_{B_0} - 19.7 \cdot \exp^{-308.5/T} \quad (2)$$

The surface tension, σ, of the different solutions were obtained using the equation proposed by Álvarez et al. [24] and Vazquez et al. [25].

3. Results and discussion

The purpose of this work is to study the variation of interfacial area in a bubble column with the time, height of the column, gas flow rate and amine physical properties. The gas holdup and the

mean Sauter diameter will be extracted by analyzing the obtained images, thus enabling a calculation of the interfacial area.

3.1. Visual observations

The images obtained for this gas–liquid system reveal that the bubble size is not constant throughout the column, the size being larger at the bottom of the column. Moreover, in the same gas–liquid system, the bubble size changes with the time in the middle and top sections of the column. This is due to the fact that the absorption process of CO_2 in aqueous DEA solutions is associated with a fast chemical reaction in the range of studied concentrations [26]; therefore, the amount of carbon dioxide absorbed and the physical properties of the liquid phase change with the time as the reaction passes.

The photographs provide visualization, according to column height, of the bubble size observed in the bubble column. The bubbles have a symmetric ellipsoidal shape. They rise almost vertically with the same speed without coalescence, drifting an amount of liquid to the top of the column. The amount of liquid carried up by the bubbles, on its way up, hinders the uprising bubbles, thus resulting in an increase of gas holdup [27].

It was observed that the bubble size does not change significantly with the time at the bottom of the column, while in the middle and in the top the bubble size increases during the process. On the other hand, when the process finishes, bubble size is practically the same in the entire column. On the other hand, this system has higher interfacial area values at the top of the column, until the saturation is reached.

In general, as the process begins, the bubble size decreases until it reaches a minimum value, increasing in size thereafter. This effect is more important at the top of the column, and less so at the bottom. Furthermore, the effect is enhanced by the amine concentration, and varies with the gas flow rate, depending on the flow regime. This could be related with changes in the physical properties. Some authors have observed that an increase in the liquid phase viscosity could have certain influence on the interfacial area [28] and consequently on the bubble size.

3.2. Bubble size

In all experiments, bubble size was calculated at three distances above the sparger surface (i.e., 20, 45 and 85 cm). Their values permit to obtain the interfacial area. The bubble shape was assumed to be oblate ellipsoidal, and the major and minor axes of the projected ellipsoid were measured using *UTHSCSA Image Tool* software.

The equivalent diameter of a sphere with the same volume as the ellipsoid was taken as the representative bubble dimension:

$$d = \sqrt[3]{E^2 e} \tag{9}$$

where E and e are, respectively, the major and minor axes of the ellipsoid in a two-dimensional projection.

The bubble size distribution was defined by the Sauter mean diameter [29]:

$$d_{32} = \frac{\sum_i n_i d_i^3}{\sum_i n_i d_i^2} \tag{10}$$

where n_i is the number of bubbles having an equivalent diameter d_i.

It is expected that the bubble size increases with increasing gas flow rate, but this only occurs in the homogeneous regime. When the diethanolamine concentration is 0.1 M (Fig. 2), the bubble size increases at low gas flow (10 and 15 L/h) and decreases at high gas flow (20 and 25 L/h). At a concentration of 0.05 M (Fig. 3), the bubble size increases with the gas flow rate. In short, the Sauter mean

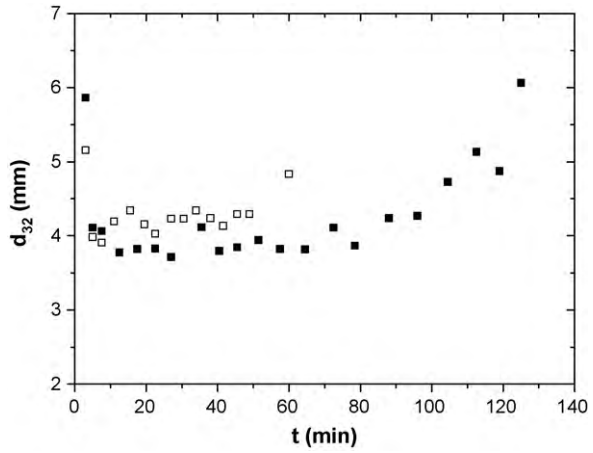

Fig. 2. Effect of reaction time on Sauter mean diameter at the top of the column at 0.1 M: Q_G = 10 L/h (■); Q_G = 15 L/h (□).

diameter decreases with amine concentration. When amine concentration increases, viscosity also increases and superficial tension decreases. The reduction in surface tension has been reported to support the maintenance if small bubbles throughout the liquid phase [30–32]. Nevertheless, the physical properties are not the sole contributing factor. The reduction in bubble size is largely attributed to changes on the flow patterns, since it is known that heterogeneous regime promotes bubble break-up [33].

3.3. Flow regime

Depending on the gas flow rate, the flow regimes observed in bubble column are the homogeneous bubbly regime encountered at low gas velocities, the heterogeneous (churn-turbulent flow) regime observed at higher velocities or the transition regimen between the homogeneous and the heterogeneous [27].

The flow regimes can be distinguished by plotting the gas holdup (ε) versus the superficial gas velocity (u_G). Hence, the gas holdup was measured using the volume expansion method which consists of visual measurements of the static liquid volume and the aerated gas–liquid dispersion volume.

$$\varepsilon = \frac{\Delta V}{\Delta V + V_L} \tag{3}$$

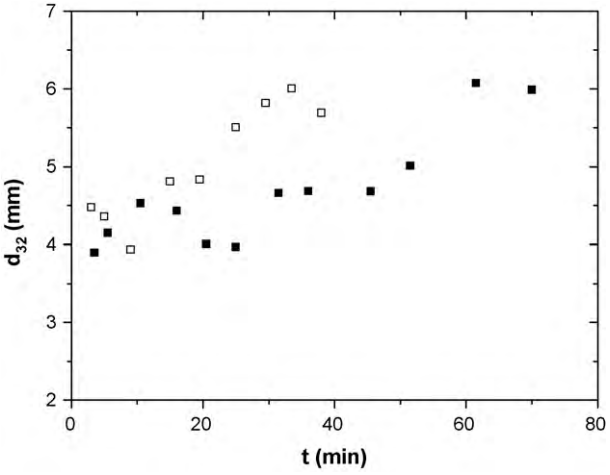

Fig. 3. Effect of reaction time on Sauter mean diameter at the top of the column at 0.05 M: Q_G = 10 L/h (■); Q_G = 20 L/h (□).

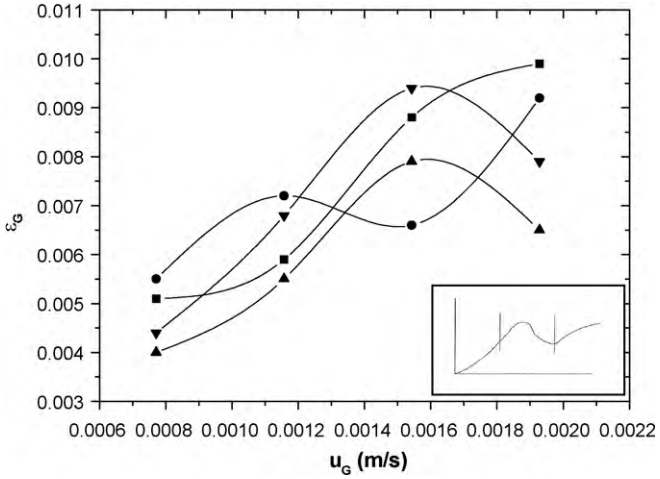

Fig. 4. Effect of DEA concentration on gas holdup: 0.05 M (■), 0.1 M (●), 0.3 M (▲) and 1.0 (▼).

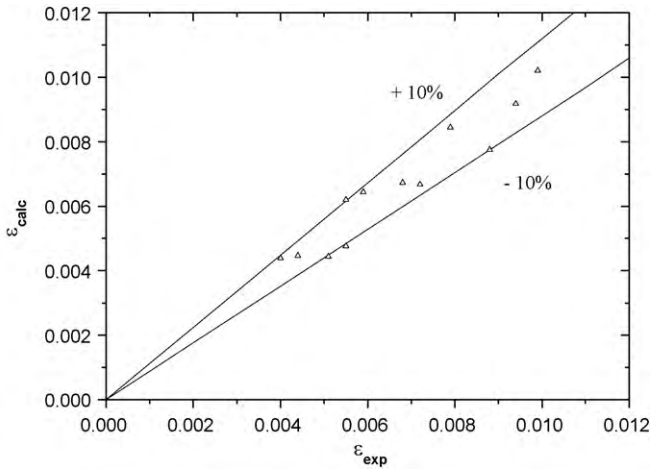

Fig. 5. Comparison of experimental ε and predicted ε.

where V_L is the ungassed liquid volume and ΔV is the volume expansion after gas dispersion, calculated from the liquid level change and the cross-sectional area. In the bubble column contactor, since the section is constant, the gas holdup is simply given by,

$$\varepsilon = \frac{\Delta H}{\Delta H + H_L} \tag{4}$$

where H_L is the ungassed liquid height and ΔH is the increase in liquid level after gassing.

Fig. 4 shows the dependence of the gas holdup on the corresponding superficial gas velocity for all systems studied. A typical flow regime map [27] is also included for comparison. In this map, the first part of the curve corresponds to the homogeneous regime where the gas holdup increases with the superficial gas velocity. A transition regime follows, where a slight decrease in gas holdup is observed. Finally, in the heterogeneous regime the gas holdup keeps increasing but with a lower slope than the homogeneous regime.

In this graphic, it is observed that the regime is always homogeneous at lower superficial gas velocity for all diethanolamine aqueous solutions. At lowest DEA concentration (0.05 M), the regime is always homogeneous with the operative gas flow rate. However, as the DEA concentration increases to 0.1 M, the regime is homogeneous at the low operation gas flow rate, reaching a heterogeneous regime at the higher flow rate. Whereas at higher DEA concentrations (0.3 and 1.0 M) and at the operation gas flow rates, the heterogeneous regime is not reached. Therefore, it can be deduced that the gas holdup depends on the liquid phase and superficial gas velocity.

To formulate a generalized correlation that would incorporate the relative effect of the physical properties of the liquid phase and operation conditions, dimensionless analysis was performed. The effect of gas velocity can be taken into account by defining the Froude (Fr) number:

$$\mathrm{Fr} = \frac{u_G}{d_C g} \tag{5}$$

where u_G is the gas superficial velocity and d_C the column diameter. Similarly, the effect of the physical properties of the liquid phase can be included in the Archimedes (Ar) and Eötvos (Eo) numbers defined as follows:

$$\mathrm{Ar} = \frac{d_C^3 \rho^2 g}{\mu^2} \tag{6}$$

$$\mathrm{Eo} = \frac{d_C^2 \rho g}{\sigma} \tag{7}$$

where μ, ρ, σ are the liquid viscosity, density and surface tension, respectively calculated with Eqs. (1) and (2) and those proposed by Álvarez et al. [24] and Vazquez et al. [25].

Finally, the ratio of mean Sauter diameter on column diameter (d_{32}/d_C) was also included to account for the different bubble size. The attempt to formulate a generalized relation that would be valid for both homogeneous and heterogeneous regimes was unsuccessful. Thus, a correlation that is valid only for the homogeneous regime was formulated for all amine concentration:

$$\varepsilon = 1.83 \cdot 10^{-9} \cdot \mathrm{Fr}^{0.45} \cdot \mathrm{Ar}^{0.62} \cdot \mathrm{Eo}^{0.7} \cdot \left(\frac{d_{32}}{d_C}\right)^{-1.3} \tag{8}$$

This correlation reveals the roles played by the different regions in the bubble column reactor. The first term represents the influence of the gas-input rate. The Ar and Eo numbers represent the influence of the physical properties, mainly viscosity and surface tension, and show a significant influence on the gas holdup, for the gas holdup range investigated in this study. The exponent of (d_{32}/d_C) is negative indicating that the Sauter mean diameter increases when the gas holdup decreases. This can be due to the effect of physical properties in the bubble size, since viscosity increases when gas holdup decreases and bubble size increases. This has been attributed to the enhanced coalescence and reduced turbulence in viscous fluids, which leads to the formation of large bubbles [34,35]. It was observed that the larger bubbles pass more quickly through the column with higher bubble rise velocities, resulting in a decreased gas holdup.

In order to test the validity of the correlations proposed for the gas holdup, Fig. 5 shows a comparison of the experimental and the predicted values of ε for all studied systems. These comparisons indicated a fairly good agreement (±10%) between the predicted and the experimental data. Moreover, this equation is similar to the correlation proposed by Mouza et al. [14] for a similar bubble column or the correlation proposed by Kilonzo et al. [36].

3.4. Interfacial area

The optimum operating conditions of a bubble column would be the ones which enhance mass transfer. This is accomplished by maximizing the gas–liquid interfacial area, which can be estimated by:

$$a = \frac{6\varepsilon}{d_{32}(1-\varepsilon)} \tag{11}$$

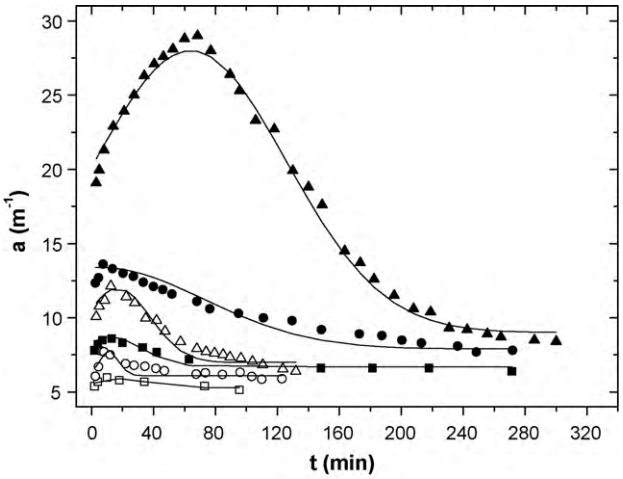

Fig. 6. Effect of the column height and concentration of DEA on interfacial area (Q_G = 15 L/h): [DEA] = 0.3 M: h = 20 cm (□), h = 45 cm (○), h = 85 cm (△); [DEA] = 1.0 M: h = 20 cm (■), h = 45 cm (●), h = 85 cm(▲); Gauss equation (—).

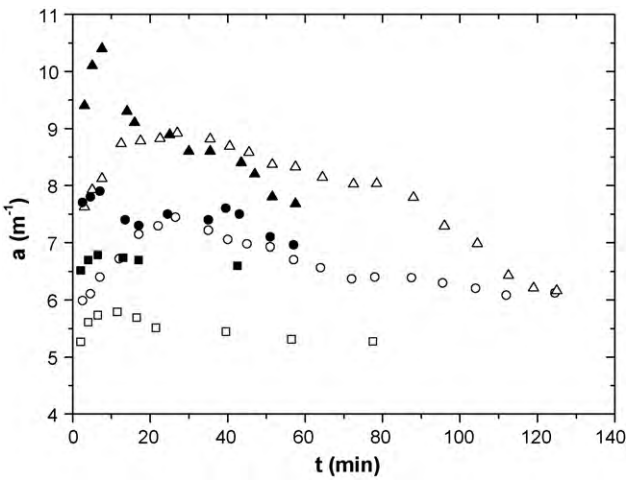

Fig. 7. Effect of the column height and gas flow rate on interfacial area ([DEA] = 0.1 M): Q_G = 10 L/h: h = 20 cm (□), h = 45 cm (○), h = 85 cm (△); Q_G = 20 L/h = 20 cm (■), h = 45 cm (●), h = 85 cm (▲).

Consequently, the homogeneous bubbly flow regime encountered at the lower gas flow rates is the most desirable for mass transfer operations. By allowing a large gas holdup value accompanied by relative bubble size, it provides a larger interfacial area.

The interfacial area was calculated at three distances above the sparger surface. In Fig. 6, the variation of the interfacial area with the operation time is presented for two different amine concentrations, and for three distances. It can be observed that higher interfacial area values are reached when the DEA concentration increases. In both cases, it seems that at 85 cm there is a high variation in the interfacial area, and it is obvious that the form of the curve changes with height. In simpler systems, like air–water, there is no variation with the height [13,14]. Moreover, since the interfacial area is defined by the Sauter mean diameter and the gas holdup according to Eq. (1), the parameters which characterise them are likely to influence the behaviour of interfacial area.

It was very difficult to develop a correlation to predict the interfacial area as a function of time and height column due to the complexity of the system. Therefore, the correlation has been developed with these variables separately. A Gauss type correlation was proposed to relate the values of the interfacial area with time for each system. The obtained parameters were related with the height column using a second order polynomial equation.

$$a = y_0 + A \cdot e^{-((t-x_C)^2/2w^2)} \quad (12)$$

where y_0 is the offset, A is the amplitude, t is the time, w the width and x_C the centre. It can be observed in Fig. 6 that the Gauss correlation adjusts the experimental results reasonably well. The range of variation of the different parameters for the correlation are:

$$2.8 < y_0 < 13.6 \quad 1.5 < w < 70$$
$$0.2 < A < 29 \quad 0 < x_C < 85$$

Thus, the interfacial area also changes with the gas flow rate (Fig. 7). Higher values of interfacial area are obtained with higher gas flow rates. As discussed earlier, the bubble diameter decreases and the gas holdup increases with the gas flow rate and, therefore, the interfacial area would increase.

In all cases, the curves suggest that the majority of the bubbles have the same size near the sparger. Upon detaching from the sparger surface, however, the bubbles do not keep their initial size. This is attributable to the chemical reaction that seems to start on the sparger surface.

Note that the specific interfacial area increases in the same way as the holdup, indicating that the increase in the bubble size with the carbon dioxide velocity, which decreases the specific interfacial area, is upset by the larger number of bubbles retained. Majumder et al. [17] observed that the interfacial area varied with the operating variables as well as the location of the column, increasing its value when the bubble diameter decreases and gas holdup increases.

4. Conclusions

The evaluation of the interfacial area in different locations of the bubble column and the influence of the gas flow rate and amine concentration were carried out. The experimental results allow concluding that the interfacial area increase as the bubble rises along the column since its size is larger at the bottom than at the top. This effect can be easily explained by the fact, that at the start of the test the CO_2 reacts rapidly with DEA solution and the bubble size shrinks on its path up. The major finding of this work is that the influence of the flow patterns and the physical properties of the liquid phase on the bubble diameter and the gas holdup becomes critical to predicting the mass transfer in aqueous diethanolamine solutions since both parameters define the gas–liquid interfacial area.

Moreover, the interfacial area varies with time in the different sections. At the bottom of the column, bubble size does not change with time considerably. Whereas at the middle and top, the bubble size decreases initially, and then, it increases until reaching a constant value in whole column. The interfacial area for each column position was fitted to Gauss equation.

A dimensional correlation has been developed to predict the gas holdup as a function of physical properties and bubble diameter, which agree well with the experimental results.

References

[1] E. Camarasa, C. Vial, S. Poncin, G. Wild, N. Midoux, J. Bouillard, Influence of coalescence behaviour of the liquid and of gas sparging on hydrodynamics and bubble characteristics in a bubble column, Chem. Eng. Process. 38 (1999) 329–344.
[2] M. Polli, M. Di Stanislao, R. Bagatin, E. Abu Bakr, M. Masi, Bubble size distribution in the sparger region of bubble columns, Chem. Eng. Sci. 57 (2002) 197–205.
[3] R. Kumar, R. Kuloor, The formation of the bubbles and the drops, Adv. Chem. Eng. 8 (1970) (1970) 255–268.
[4] N. Rabiger, A. Vogelphol, Bubble formation and its movement in Newtonian and non-Newtonian liquids, in: N.P. Cheremisinoff (Ed.), Encyclopedia of Fluid Mechanics, vol. 3, Gulf Publishing Company, Houston, USA, 1986, p. 58.

[5] H. Tsuge, Hydrodynamics of bubble formation from submerged orifices, in: N.P. Cheremisinoff (Ed.), Encyclopedia of Fluid Mechanics, vol. 3, Gulf Publishing Company, Houston, USA, 1986, p. 191.
[6] T. Miyahara, Y. Matsuba, T. Takahashi, The size of bubbles generated from perforated plates, Int. J. Chem. Eng. 23 (1983) 517–523.
[7] J.M. Delhaye, J.B. McLaughlin, Appendix 4: report of study group on microphysics, Int. J. Multiphase Flow 29 (2003) (2003) 1101–1116.
[8] K. Akita, F. Yoshida, Bubble size, interfacial area, and liquid phase mass transfer coefficients in bubble columns, Ind. Eng. Chem. Process Des. Dev. 13 (1974) 84–91.
[9] M. Millies, D. Mewes, Phase boundaries in bubble flow. Part 1. Bubble column, Chem. Ing. Technol. 68 (1996) 660–669.
[10] T. Miyahara, T. Hayashino, Size of bubbles generated from perforated plates in non-Newtonian liquids, J. Chem. Eng. Japan 28 (1995) 596–600.
[11] J. Varley, Submerged gas–liquid jets: bubble size prediction, Chem. Eng. Sci. 50 (1995) 901–905.
[12] T. Miyahara, A. Tanaka, Size of bubbles generated from porous plates, J. Chem. Eng. Japan 30 (1997) 335–355.
[13] D. Colella, D. Vinci, R. Bagatin, M. Masi, E. Abu Bakr, A study on coalescence and breakage mechanism in three different bubble columns, Chem. Eng. Sci. 54 (1999) 4767–4777.
[14] A.A. Mouza, G.K. Dalakoglou, S.V. Paras, Effect of liquid properties on the performance of bubble column reactors with fine pore spargers, Chem. Eng. Sci. 60 (2005) 1465–1475.
[15] T. Otake, S. Tone, K. Nakao, Y. Mitsuhashi, Coalescence and break-up of bubbles in liquids, Chem. Eng. Sci. 32 (1977) 377–383.
[16] K.L. Tse, T. Martin, C.M. McFarlane, A.W. Nienow, Small bubble formation via coalescence dependent break-up mechanism, Chem. Eng. Sci. 58 (2003) 275–286.
[17] S.K. Majumder, G. Kundu, D. Mukherjee, Bubble size distribution and gas–liquid interfacial area in a modified downflow bubble column, Chem. Eng. J. 122 (2006) 1–10.
[18] J.E. Botello-Álvarez, J.L. Navarrete-Bolaños, H. Jiménez-Islas, A. Estrada-Baltazar, R. Rico-Martínez, Improving mass transfer coefficient prediction in bubbling columns via sphericity measurements, Ind. Eng. Chem. Res. 43 (2004) 6527–6533.
[19] M. Laakkonen, M. Honkanen, P. Saarenrinne, J. Aittamaa, Local bubble size distributions, gas–liquid interfacial areas and gas holdups in a stirred vessel with particle image velocimetry, Chem. Eng. J. 109 (2005) 37–47.
[20] R. Lemoine, A. Behkish, B.L. Morsi, Hydrodynamic and mass-transfer characteristics in organic liquid mixtures in a large-scale bubble column reactor for the toluene oxidation process, Ind. Eng. Chem. Res. 43 (2004) 6195–6212.
[21] J.M.T. Vasconcelos, J.M.L. Rodrigues, S.C.P. Orvalho, S.S. Alves, R.L. Mendes, A. Reis, Effect of contaminants on mass transfer coefficients in bubble column and airlift contactors, Chem. Eng. Sci. 58 (2003) 1431–1440.
[22] J.M.T. Vasconcelos, S.P. Orvalho, S.S. Alves, Gas–liquid mass transfer to single bubbles: effect of surface contamination, AIChE J. 48 (2002) 1145–1154.
[23] L.D.C. Correia, C. Aldrich, K.G. Clarke, Interfacial gas–liquid transfer area in alkane-aqueous dispersions and its impacto on the overall volumetric oxygen transfer coefficient, Biochem. Eng. J. 49 (2010) 133–137.
[24] E. Álvarez, R. Rendo, B. Sanjurjo, M. Sanchez-Vilas, J.M. Navaza, Surface tension of binary mixtures of water + N-methyldiethanolamine and ternary mixtures of this amine and water with monoethanolamine, diethanolamine, and 2-amino-2-methyl-1-propanol from 25 to 50 °C, J. Chem. Eng. Data 43 (1998) 1027–1029.
[25] G. Vázquez, E. Álvarez, R. Rendo, E. Romero, J.M. Navaza, Surface tension of aqueous solutions of diethanolamine and triethanolamine from 25 °C to 50 °C, J. Chem. Eng. Data 41 (1996) 806–808.
[26] R. Maceiras, Absorción de dióxido de carbono en disoluciones acuosas de alcanolaminas: Aplicación de Técnicas electroquímicas, PhD Thesis, University of Vigo, Spain, 2006.
[27] M. Ruzicka, J. Zahradnik, J. Drahos, N.H. Thomas, Homogeneous–heterogeneous regime transition in bubble columns, Chem. Eng. Sci. 56 (2001) 4609–4626.
[28] D. Gómez-Díaz, J.M. Navaza, L.C. Quintáns-Rivero, B. Sanjurjo, Gas absorption in bubble column using a non-Newtonian liquid phase, Chem. Eng. J. 146 (2009) 16–21.
[29] Y.T. Shah, B.G. Kelkar, S.P. Godbole, W.D. Deckwer, Design parameters estimations for bubble column reactors, AIChE J. 28 (1982) 353–379.
[30] B.H. Junker, Measurement of bubble and pellet size distributions: past and current image analysis technology, Bioprocess Biosyst. Eng. 29 (2006) 185–206.
[31] S.A. Zieminski, M.M. Caron, R.B. Blackmore, Behaviour of air bubbles in dilute aqueous solutions, Ind. Eng. Chem. Fundam. 6 (1967) 233–242.
[32] J.A.C. van de Donk, R.G.J.M. van der Lans, J.M. Smith, Effect of contaminants on the oxygen transfer rate achieved with a plunging jet contactor, BHRA Fluid Eng. (1979) 289–302.
[33] J.L. Rols, J.S. Condoret, C. Fonade, G. Goma, Mechanism of enhanced oxygen transfer in fermentation using emulsified oxygen-vectors, Biotechnol. Bioeng. 35 (1990) 427–435.
[34] S.J. Arjunwadkar, K. Saravanan, P.R. Kulkarni, A.B. Pandit, Gas–liquid mass transfer in dual impeller bioreactor, Biochem. Eng. J. 1 (1998) 99–106.
[35] M. Nocentini, D. Fajner, G. Pasquali, F. Magelli, Gas–liquid mass transfer and holdup in vessels stirred with multiple Rushton turbines: water and water–glycerol solutions, Ind. Eng. Chem. Res. 32 (1993) 19–26.
[36] P.M. Kilonzo, A. Margaritis, M.A. Bergougnou, Hydrodynamics and mass transfer characteristics in an inverse internal loop airlift-driven fibrous-bed reactor, Chem. Eng. J. 157 (2010) 146–160.